

NUMERICAL IMPACT OF TOOL GEOMETRY ON HIP PROSTHESIS FORMING

Mondher Nasri^{1*}, Houda Khaterchi², Atef Boulila³, Olivier Dalverny⁴, Naoufel Fares⁵, Youssef Trimech⁶, Ali Zghal⁷, and Khalil Hajlaoui⁸

1.3 & 7 University of Tunis, LMPE, ENSIT, 5 Avenue Hussein, BP 56, Bâb Manara, 1008, Tunisia.
 2 University of Monastir, Mechanical Engineering Laboratory, National Institute of Engineers of Monastir, Tunisia.
 4 University of Toulouse, UTTOP, ENIT, France.
 5.6 Higher Institute of Technology Studies (ISET), Ksar Hellal, Tunisia.
 8 College of Engineering, Imam Mohammad Ibn Saud Islamic University (IMSIU), Riyadh, Kingdom of Saudi Arabia.

Abstract

This paper examines the effect of incremental forming parameters on the process of a 304L stainless-steel biomedical part, which is inserted between the prosthesis and the cup to minimize wear and extend the lifespan of the prosthesis. The methodology involves several steps. First, the tool trajectory is determined. Then, modeling and numerical simulation are performed to select the optimal configuration, evaluate the final product geometry and forming tool force in relation to the forming angle, define the forming tool dimensions, and determine the axial step. Finally, the evaluation of the spring-back is conducted, along with an analysis of the parameters that influence the thinning of the component. The results highlight the relationship between punch diameter and axial displacement on the geometric quality of the deformed component. Furthermore, the force exerted varies as a function of axial steps, forming tool geometry, and the dimensions of the deformed component. Additionally, the number of contact points and the forming angle have an impact on the thinning.

Keywords: SPIF, Thin plate, Total hip replacement (THR), Sensitivity analysis, Finite Element Method

1. Introduction

The total hip prosthesis is a medical device used to replace the damaged or worn hip joint. It is made up of several components, including a metal, ceramic or polymer cup that is fixed in the acetabulum of the pelvic bone, a metal stem inserted in the femur, and a spherical metal or ceramic head that articulates with the cup. Currently, the primary issue is wear between the cup and the prosthetic head (Fig. 1). There are many types of prostheses available, with a range of sizes to suit almost any hip shape. The choice of prosthesis size depends on several parameters, including cup wear, manufacturing material, and the risk of dislocation. To reduce the friction, the diameter of the prosthesis head should be small, generally between 22 mm and 28 mm [1-3]. However, reducing the diameter below 22 mm increases the risk of dislocation. Various material combinations are used to minimize the expenses associated with producing the prosthesis. The metal-metal pair is the least worn but also the most expensive, while the ceramic-ceramic pair is less expensive but more complex to manufacture. The metal-plastic pair is subject to wear but is easier to manufacture and less expensive than the other pairs. To

minimize wear and extend the prosthesis's life, a stainless-steel insert can be used. This reduces wear and improves the durability of the prosthesis. In this context, a study is being conducted to develop a manufacturing process for a component to be inserted into the cup and head of the prosthesis, aiming to reduce wear and optimize prosthesis performance. The sheet metal forming process has recently become an increasingly crucial element in the manufacturing process. A specific technique, known as Single Point Incremental Forming (SPIF), has garnered considerable interest due to its flexibility and ability to produce small components and prototypes. [4, 5]. It has also found applications in the creation of personalized prosthetics and implants for patients [6]. Unlike traditional forming methods that involve large-scale deformation in a single operation, incremental forming achieves the desired shape through a series of localized deformations. This makes SPIF particularly interesting for cost-effective production of complex-shaped parts [7, 8]. In the incremental forming process, the sheet material is clamped at its edges while a hemispherical tool applies forces to progressively deform it [9]. The tool follows a predefined path, incrementally displacing the material to achieve the desired shape. CNC machines are commonly used for this

 $*Corresponding\ Author\ -E\text{-}mail:\ mondher.nasri@yahoo.fr$

process, providing precise control over the forming parameters [6, 10]. The parameters such as depth of pass, tool diameter, sheet thickness, coefficient of friction, type of lubricant, tool path, and wall angle have a crucial role on the quality, dimensional accuracy, and durability of the final part [11],[12, 13]. While manufacturers typically utilize highly formable materials, such as aluminum alloys, for incremental forming processes [14, 15], there have been numerous studies investigating the forming of other material types like Titanium [16], PVC [17], magnesium alloys [18] or composite [19]. Besides, stainless steel 304L has been the focus of several research studies due to its exceptional mechanical properties, high corrosion resistance, and low susceptibility to oxidation [11, 17]. The effects of different parameters on forming results need to be studied and clarified to improve the incremental forming process and ensure the desired quality of the final product. Substantial research has been conducted in recent years to investigate the impact of these parameters on the process. Numerical simulations, experimental studies, and analytical modeling have been employed to gain insights into the complex interactions between the process parameters and the resulting part characteristics. These studies have yielded valuable findings and guidelines for process optimization; however, there is still room for further exploration and understanding. Bensaid et al. [4] carried out finite element simulations of the single-point incremental forming (SPIF) process to produce a truncated cone. They studied the impact of tool geometry and sheet properties on forming force, stress distribution, and sheet thinning. They observed that sheet thinning was more pronounced in the case of a continuous tool path than in the case of a discontinuous tool path. Chennakesava [11] focuses his research on the finite element modeling of the single-point incremental sheet forming (SPIF) process, utilizing Stainless Steel 304 and incorporating elliptical geometry. Experimental trials were carried out using a CNC machine, and the results obtained were verified through finite element analysis. The formability of 304 stainless steel elliptical cups is significantly influenced by key factors, including sheet thickness, pass depth, and tool radius. Saidi et al. [6] studied the impact of four parameters (sheet thickness, punch diameter, pitch size, and wall angle) on maximum forming force using an experimental design. In a related context, Ambrogio et al. [18] observed that forces involved in incremental forming are influenced by various factors, including tool dimensions, vertical step, sheet thickness, and forming wall angle. Several studies [10, 18] have explored the effects of vertical increment, tool diameter, and rotational speed on the forming force. Additionally, other researchers have highlighted the potential of adjusting

rotational speed and using lubricants to reduce the forming force during the incremental forming process [10, 20, 21]. This article aims to contribute to the existing body of knowledge by presenting a comprehensive study of the effect of different parameters on the incremental forming process in the production of hip prosthesis cups. Using numerical simulations, we aim to assess the influence of punch diameter, axial step size, and tool path strategy on forces, springback behavior, and material thinning. In this study, analysis of variance (ANOVA) is used to identify the input parameters that minimize the maximum forming force. By varying these parameters and analyzing the results obtained, we aim to provide valuable insights that can guide process design and optimization in incremental forming applications. The results presented in this article can serve as a basis for optimizing the incremental forming process, enhancing part quality, and expanding the range of applications for this promising manufacturing technique.

2. Method of incremental sheet forming processes

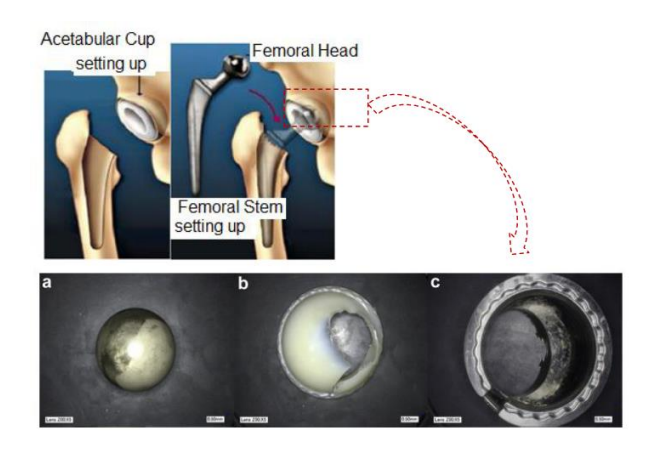


Fig. 1: Hip prosthesis: Assembly of total, (a,b c) Wear of polyethylene cup by metal head [22, 23]

Incremental forming is a process that shapes a sheet of metal by applying successive local deformations and incrementally applying pressure to the sheet with a small hemispherical tool (usually with a diameter ranging from 4 mm to 10 mm) that traverses the sheet's surface. The success of producing a part lies in the ability to evenly distribute deformations throughout the entire niece while avoiding excessive deformation concentration in specific areas. The path followed by the punch is crucial as it dictates the formability of a component, signifying its capability for undergoing deep drawing processes. This trajectory depends on the

increments chosen for the punch. Fig. 2 illustrates this principle by showing the vertical increments (Δz) and the horizontal increments $(\Delta x, \Delta y)$, which depend on the type of loading. The punch can be fixed, free, or imposed in rotation.

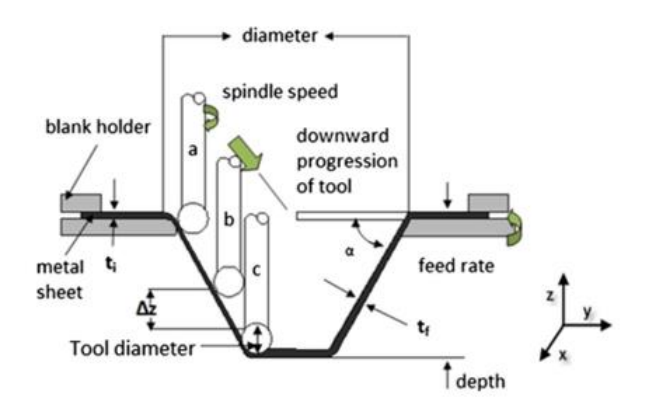


Fig.2: Schematic illustration of the SPIF method [24]

3. Determination of the forming tool path

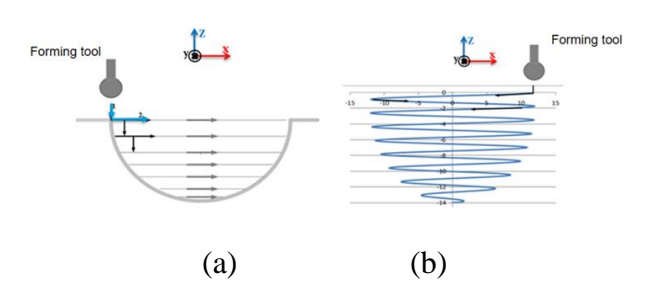


Fig. 3: Two types of tool trajectories: a) discontinuous — vertical increment along the Z-axis followed by a combined displacement in X and Y directions $(\Delta x, \Delta y)$; b) Continuous — simultaneous displacement along all three axes $(\Delta x, \Delta y, \Delta z)$.

There are various toolpath strategies for the incremental forming process, which can be either continuous or discontinuous [25]. The geometry of the final product will determine the choice of forming tool path as well as the dimensions of the step increments (Δx , Δy and Δz), which is directly influenced by the geometry of the final product. Indeed, the continuity of motion enhances the surface condition of the part throughout its forming process. Figs. 3 illustrate two types of tool path generation: discontinuous or continuous. The

discontinuous path consists of a sequence of contours created along the axis of the hemisphere (Figs. 3.a). Initially, the tool descends into the sheet over a distance corresponding to the specified axial step, as indicated with arrow 1. It then traverses the circular contour in the direction of arrow 2. As soon as the contour path is completed, the tool must shift horizontally by a step size Δx and then axially by a step size Δz to proceed to the next contour. The continuous trajectory of the tool implies an uninterrupted variation of its motion in x, y and z so as to describe the surface to be created (Figs. 3.b).

Several studies have examined the impact of continuous versus discontinuous toolpaths in the incremental forming of metal parts, and several significant conclusions have been drawn [26, 27]:

- i. Part quality: Research indicates that continuous toolpaths lead to more regular deformations and more homogeneous stress distribution. This translates into a significant improvement in the quality of the final part [28].
- ii. Cycle time reduction: By optimizing continuous trajectories it is possible to reduce forming cycle times while maintaining high quality levels. This approach is particularly advantageous in high-speed production processes.
- iii. Minimization of surface defects: Continuous trajectories help to reduce the risk of marking and excessive deformation of the part surface. This significantly improves the aesthetics functionality of formed parts [29] . Another comparative study has shown that discontinuous paths can give rise to various problems, such as transition marks, local stress build-up and less homogeneous strain distribution. This can affect the quality and durability of formed parts [30]. In this study, we opted for a continuous trajectory for the biomedical part. The tool path was generated using CATIA software and programmed with MATLAB code.

3.1. Analytical modeling

The complexity of defining the tool path trajectory increases with increasing intricacy of the final workpiece geometry and the necessity to decrease the increment size. To address this challenge, we devised a trajectory outlining the final product's geometry using a conventional approach that involves manually computing a hemispherical shape based on the hip prosthesis (PTH). The tool moves in the horizontal plane (X, Y) following

an Archimedean spiral, while axial displacement is required to achieve the spherical shape by adjusting the spiral's radius.

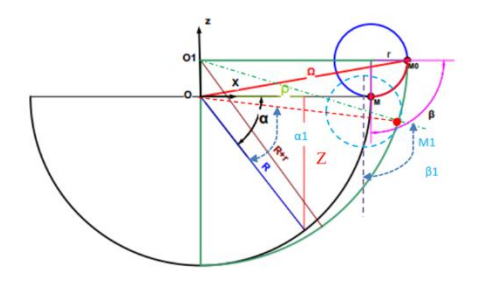


Fig. 4: Spherical trajectory without correction

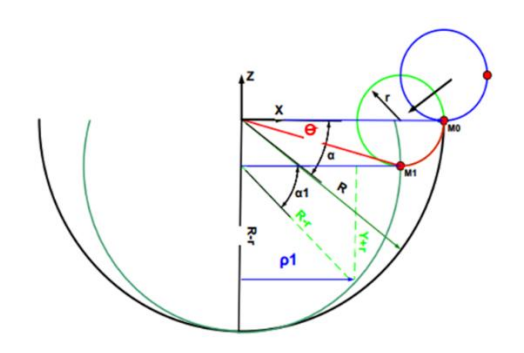


Fig. 5: Spherical trajectory with correction

Fig. 4 illustrates the uncorrected spherical trajectory of the tool. The expression determining the variation in spiral radius is provided as follows:

$$\rho = R\cos\alpha \tag{1}$$

With is the axial displacement angle, is the spire radius, and is the Axial step. The coordinates form the trajectory (in black) of the tool driven by point M with the coordinates $X = \rho Cos(\theta)$, $Y = \rho Sin(\theta)$ and Z. (θ) here is the angle of rotation in the horizontal plane Z. The trajectory (in green) of the contact point M_0 is shown in the vertical plane with the coordinates:

$$X = R\cos(\alpha) + r\sin(\beta),$$

 $Z = R\sin(\alpha) + r\sin(\beta)$. $\beta = (\frac{\pi}{2} - \alpha)$,, hich forms a circle with the equation: $X^2 + (Z - r)^2 = (R - r)^2$. We notice that the dimensions of the piece are larger than the desired shape, which requires correction. We use the inverse method to find the trajectory of point M_1 , which guides the tool, in the (X, Z) plane with the coordinates

$$X_1 = R\sin(\alpha_1) - r\sin(\beta_1),$$

$$Z_1 = R\sin(\alpha_1) - r\sin(\beta_1)$$

Fig. 5, which represents a circle of equation $X^2 + (Z + r)^2 = (R + r)^2$.

The corrected radius of the spiral $\rho 1$ is defined by the following expression:

$$\rho_1 = (R - r)\cos(\alpha_1) \tag{2}$$

Where $\alpha_1 = \arcsin\left(\frac{Z_1 + r}{R - r}\right)$. The coordinate of

point M_1 that controls the tool is $X_1 = \rho_1 \cos(\theta)$, $Y_1 = \rho_1 \sin(\theta)$.

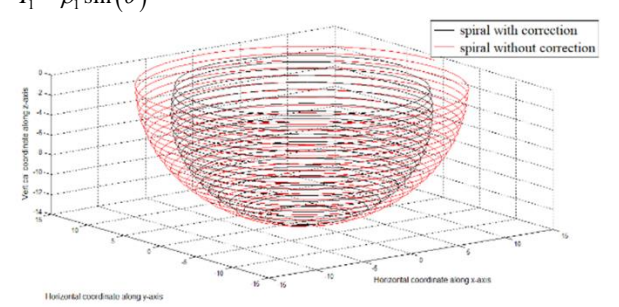


Fig. 6: Spherical trajectory with correction and without correction

Fig. 6 illustrates two configurations, with and without tool path correction.

3.2. Numerical method

In the industry context, parts are typically designed using CAD (Computer-Aided Design) software. To guarantee robust and accurate simulations, it is essential to drive these simulations from topologies created in CAD and tool paths generated using integrated CAM (Computer Aided Manufacturing) tools. However, the main CAM software packages are generally designed to define machining strategies based solely on geometric criteria and are not directly compatible with numerical finite element simulation codes. In our case, we used CATIA V19 to create trajectories. Figs. 7 and 8 illustrate the program loading steps for tool path execution and the result of the numerical model of the spherical part studied, produced using a circular path during the incremental forming process.

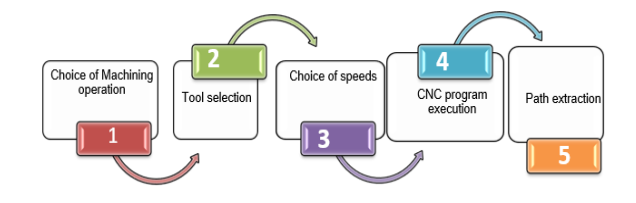


Fig. 7: Workflow diagram of the tool control path generation procedure

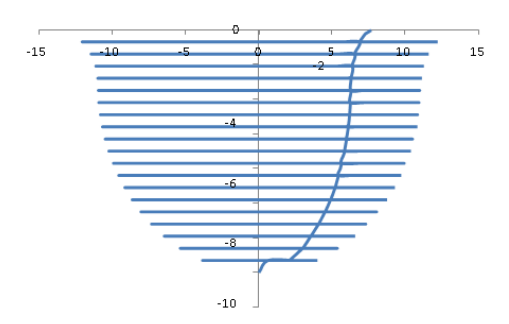


Fig. 8: Result of the simulated trajectories in CATIA V5R19

4. Numerical Simulation of SPIF

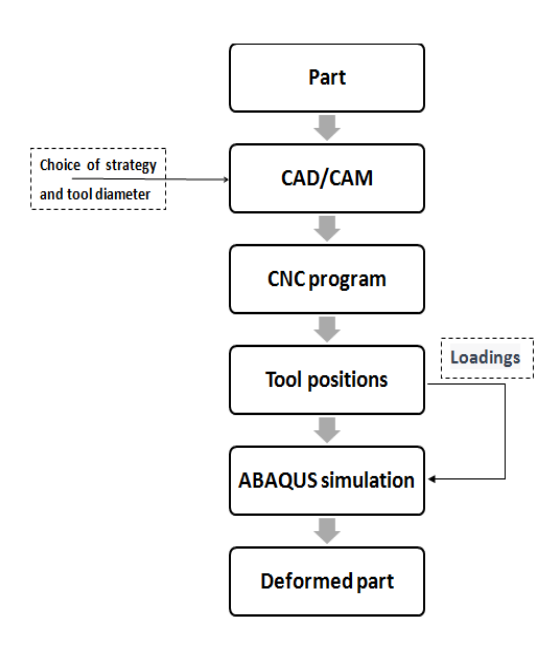


Fig. 9: Flowchart of numerical modeling

Numerical simulation currently represents a favored tool in product design. It also examines the feasibility of forming operations and reduces the number of experiments required for process optimization and tool design. The digital chain developed transfers the trajectories generated in the CAD/CAM environment of the CATIA software to the ABAQUS calculation code (Fig. 9). This section focuses on the numerical simulation of the incremental forming process of a circular plate, with particular emphasis on the analysis of the forces exerted by the tool. Additionally, the aim is to determine the parameters of the incremental forming process that enable us to evaluate the final form of the piece.

4.1. Geometric model configuration

selected geometry for the numerical encompasses investigation hemispherical a configuration, characterized by a diameter D = 28 mm(predetermined by the cup diameter of the prosthesis). Initially, prior to any deformation, the sheet material assumes a circular form, with dimensions denoting a free zone diameter of D and an equable thickness of 1 mm (excluding consideration of the area under the blank holder). The tool has a hemispherical shape with a variable diameter, depending on the prescribed test parameters of 4, 6, 10 mm. Meanwhile, the die and the blank holder adopt a circular and perforated design, with a height of H = 10 mm, an external diameter of D = 100 mm, and an internal diameter corresponding to a semicircular measure of 28 mm. In particular, the rigid body assumption is used to model the forming tool, the die, and the blank holder (Fig. 10).

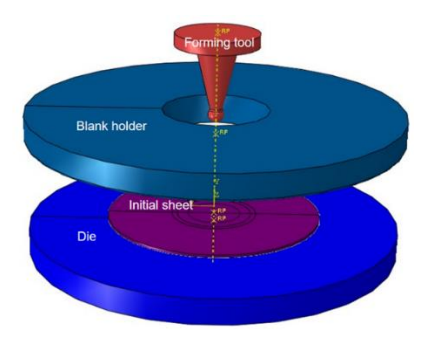


Fig. 10: Geometric model of the incremental forming process

4.2. Material Characterization of the sheet metal

An isotropic elastoplastic model associated with the von Mises plasticity criterion has been adopted to describe the material behavior. Previous work has demonstrated that 304L stainless steel, a material with low anisotropy, has been implemented in simulation software for an SIF (Sheet Incremental Forming) process. Work hardening behavior is assumed to be isotropic and is described by Swift's power law:

$$\sigma(\varepsilon) = K(\varepsilon_0 + \varepsilon^p)^n \tag{3}$$

Where σ is the equivalent stress, ϵ_p is the equivalent plastic strain, K= 1506 MPa, n= 0.5842 and ϵ_0 =0.049 represent the hardening parameters[4]. The material properties are provided in Table 1.

Table 1. Mechanical Properties of stainless steel 304L [4]

Material properties	values	
Е	200000 MPa	
ν	0.3	
Re	265 MPa	

4.3. Boundary conditions and Mesh generation

The ABAQUS explicit solver was used to perform a three-dimensional finite element analysis (FEA) of SPIF. In this simulation, the following boundary conditions were applied:

- i. Die: Permanently fixed in place.
- ii. Forming Tool: Moves along a pre-defined direction to form the desired geometry.
- iii. Sheet metal: Completely free.
- iv. Blank holder: Moves axially to hold the blank in place.

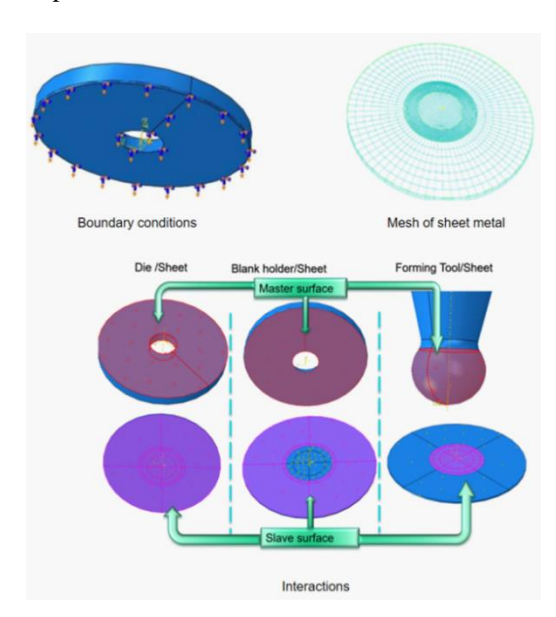


Fig. 11: Finite element component of SPIF: Boundary conditions, Mesh of sheet metal and Interactions of elements

The mesh used for the sheet is composed of C3D8R linear hexahedral elements with reduced integration. The tool, blank, and blank holder are meshed with rigid R3D4 elements, totaling 720 elements. Similarly, the die and

blank holder are meshed with R3D4 elements, totaling 528 elements. Fig. 11 details the mesh, the boundary conditions of the numerical model, and the interactions between the elements, including friction coefficients set at 0.1. The loading was applied at a displacement speed of 2 mm/min. The detailed implementation of the numerical model is shown in Fig. 11:

4.4 Systematic Parameter Exploration: Design of Experiment

Experimental design plays a crucial role in optimizing processes and systems by systematically exploring the effects of various factors and their interactions. Specifically, in the context of simulations for incremental forming, the use of a well-designed experimental plan, such as Taguchi L9 (3^2), offers a structured approach to efficiently investigate the impact of parameters, including tool diameter (mm) and axial pitches (mm), on the forming process. By systematically varying these parameters at multiple levels, experimental design enables us to gain comprehensive insights into their effects on the outcome of the forming process, thereby facilitating the identification of optimal settings. Regarding the control strategy, a continuous approach was employed for all simulations. For each variable, Tool diameter and Axial steps, three levels are considered, as presented in the following table:

Table 2: Input data

Parameters	Values	
Tool diameter (mm)	4-6-10	
Axial steps (mm)	0.5 - 0.7 - 1	

Furthermore, the reaction force on the forming tool is measured using FE simulation. This enables an exhaustive analysis of the forming process, evaluating the relationship between process parameters and the forces exerted by the tool. These forces are indicative of the material's deformation and the interaction between the tool and the piece.

5. Results and discussions

5.1. Evolution of the geometry of the final part

The aim of finite element (FE) simulation is to study and evaluate the impact of key parameters in incremental sheet metal forming (SPIF), such as tool geometry, vertical pitch, and tool forming strategy, on the evolution of forming force, final part geometry, sheet metal thinning, and springback evolution.

Effect of forming tool diameter on the final part geometry.

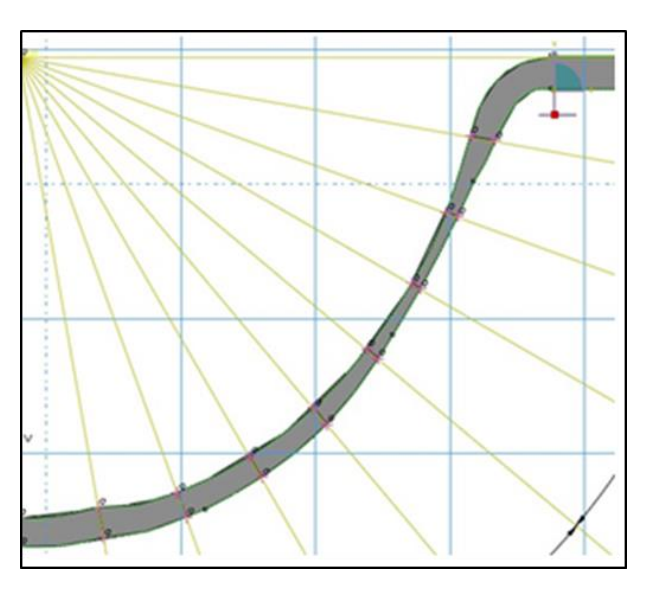


Fig. 12: ½ Visualization of the positioning of radii and thicknesses

The diameter of the forming tool has been proven to be one of the most influential parameters in simulating the incremental forming process. Actually, three different forming tool diameters were used: 4 mm, 6 mm, and 10 mm. Fig. 12 shows the method used to measure radius dimensions at 10-degree intervals. Fig. 13 shows the radius of the final product obtained at different tool diameters for a constant axial step of 0.5, 0.7, and 1 mm. To quantify the deviations between the part obtained and the part simulated by numerical software (ABAQUS), Ambrogio et al. [20] have used the square root of the average deviation, known as the Root Mean Square Error (RMS).

$$RMS = \sqrt{\frac{\sum (r_i - r_0)^2}{N_R}} ,$$

where r_i is the current radius, r_0 is the desired radius (14 mm), and N_R is the number of radius.

The variation in forming tool diameter was found to have no significant effect on the final part geometry, except for the combination of a 6 mm tool

diameter and a 0.7 mm pitch, which showed the minimum error.

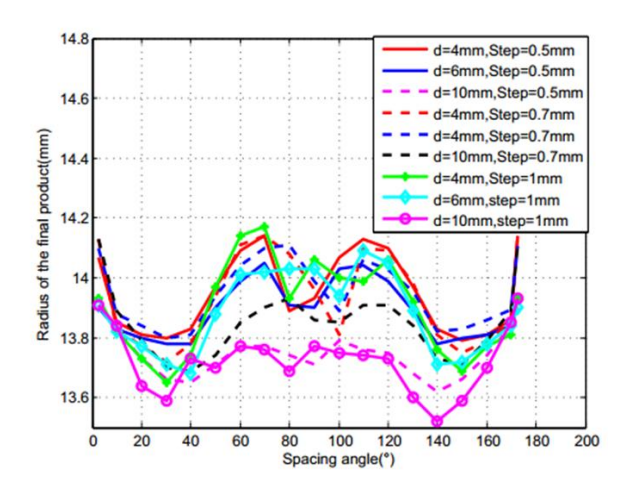


Fig. 13: Variation of the radius of the final product for a constant axial step [0.5 mm, 0.7 mm, 1 mm] with varying forming tool diameter (4, 6, 10 mm).

Table2. Reconstruction error for each diameter and axial step ratio

Test	Axial step (mm)	Diameter and axial step ratio	RMS
1	0.5	8	0.13745813
2	0.5	12	0.14164448
3	0.5	20	0.2635187
4	0.7	5.71	0.16354623
5	0.7	8.57	0.12731126
6	0.7	14.28	0.18826074
7	1	4	0.18004385
8	1	6	0.1731139
9	1	10	0.16314089

Effect of axial step depth on the final part geometry.

A numerical study was presented that focuses on the influence of varying the axial step depth on the geometry of the final part. We varied this depth at three dimensions [0.5, 0.7, and 1 mm]. The outcomes from the numerical simulation concerning the variation in axial step demonstrate no discernible impact on the geometry of the final product Figs. (14,15,16).

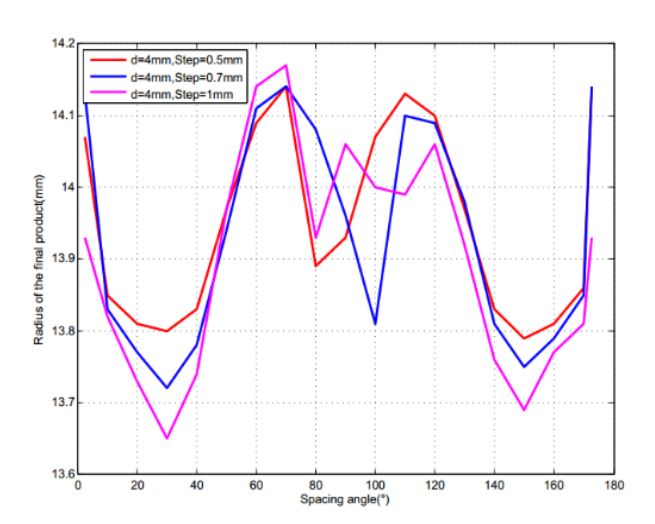


Fig. 14: Variation of the radius of the final product for a varying axial step [0.5 mm, 0.7 mm, 1 mm] with a constant forming tool diameter 4.

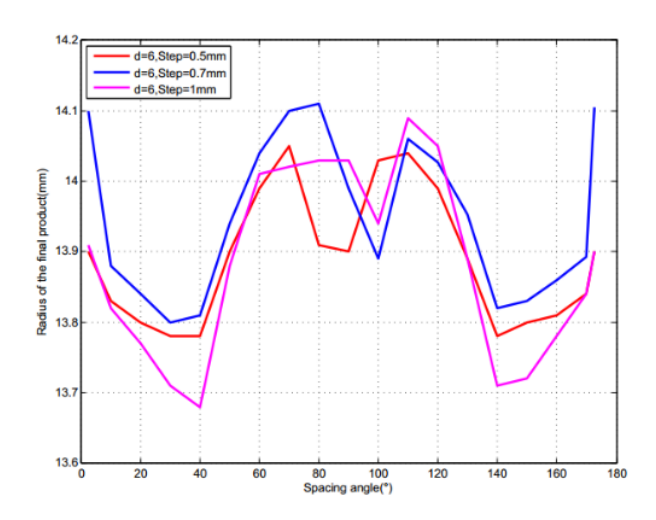


Fig. 15: Variation of the radius of the final product for a varying axial step [0.5 mm, 0.7 mm, 1 mm] with a constant forming tool diameter of 6.

5.2. Evolution of forming forces

In this part, we analyze the effect of axial pitch depth on the distribution of forces applied by the punch. The parameter Δz , representing the axial step depth, plays a crucial role in simulating the incremental forming process, as it influences the forces applied by the tool. This influence is particularly evident in the values of the maximum amplitudes of the resulting loads, as presented in Table 3 and depicted in Figs. (17,18,19). During the numerical simulations, the increment sizes along the

axial z-axis are maintained at constant values Δ , z = [0.5, 0.7, and 1 mm], and the forming tool diameter is varied to values of 4, 6, and 10 mm.

Subsequently, through the application of ANOVA, the importance of main influences and potential interactions between these variables (Tool diameter and Axial steps) can be quantitatively evaluated, guiding the optimization efforts towards achieving superior performance and efficiency in incremental forming simulations. The various combinations of these parameters are used in finite element (FE) simulations to verify the variation in forming force, and the results are presented in Table 3.

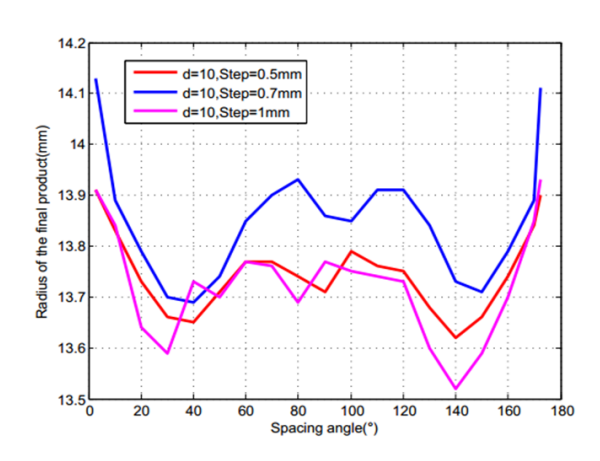


Fig. 16: Variation of the radius of the final product for a varying axial step [0.5 mm, 0.7 mm, 1 mm] with a constant forming tool diameter (4, 6, 10 mm).

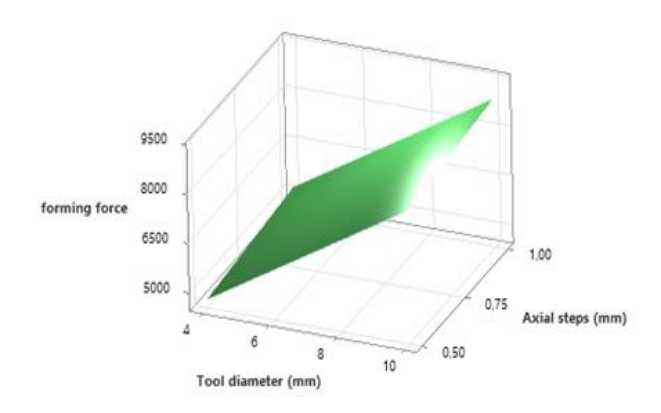


Fig. 17 Surface plot of forming force and Axial steps (mm); Tool diameter

The surface plot illustrating the variation in forming force as a function of different process

parameters (axial pitch and tool diameter) is shown in Fig. 17. This figure indicates that the maximum force increases with increasing tool diameter. It also shows that the forming force increases with higher values of axial pitch and tool diameter.

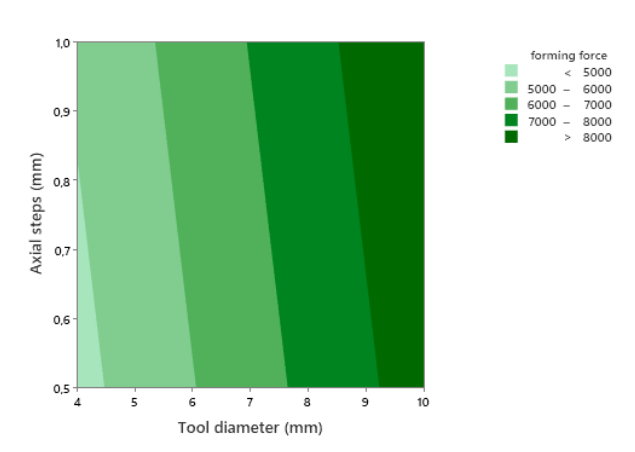


Fig. 18: Contour plot of forming force and Axial steps (mm); Tool diameter

The 2D response surface is shown in Fig. 18, representing a combination of an infinite number of possible solutions for the two factors affecting the response. Fig. 18 shows that the forming force was maximum with the highest tool diameter.

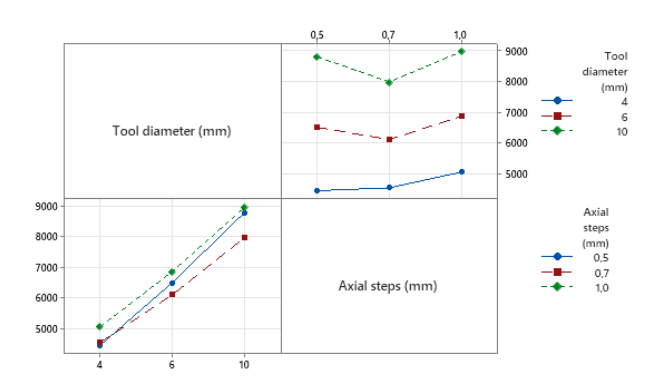
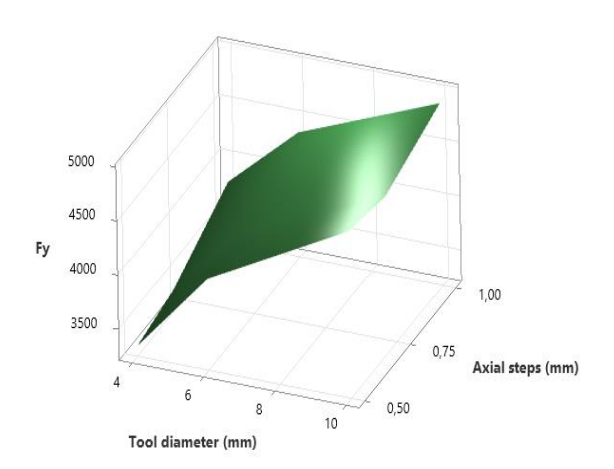
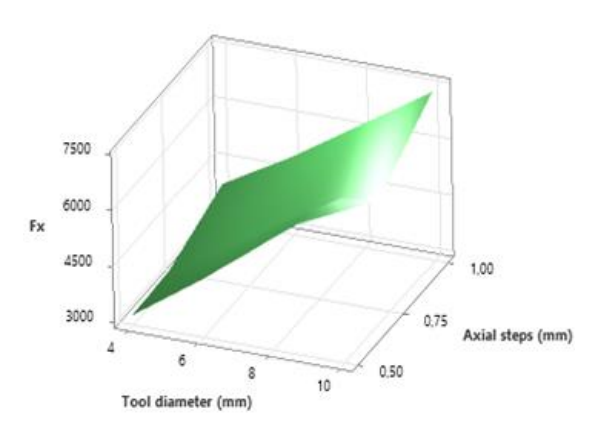


Fig. 19: Interaction plot for forming force

Furthermore, the interaction diagrams in Fig. 19 clearly show that the combination of tool diameter and axial step has a significant influence on forming force. Additionally, it was observed that the formed component size increases with higher tool diameter and larger axial steps. The increase in force with steps is minimal, and even for a pitch of 0.7 with d=6 and 10 mm, a slight decrease is observed. In Fig. 20, the interaction plots clearly indicate that the components Fx, Fy, and Fz

increase with the tool diameter. Regarding the components in Fig. 21, we have a decreasing order of Fx, Fy, and Fz. Generally, the component increases with the axial steps, except for $d=10\ mm$ and steps $=0.7\ mm$.





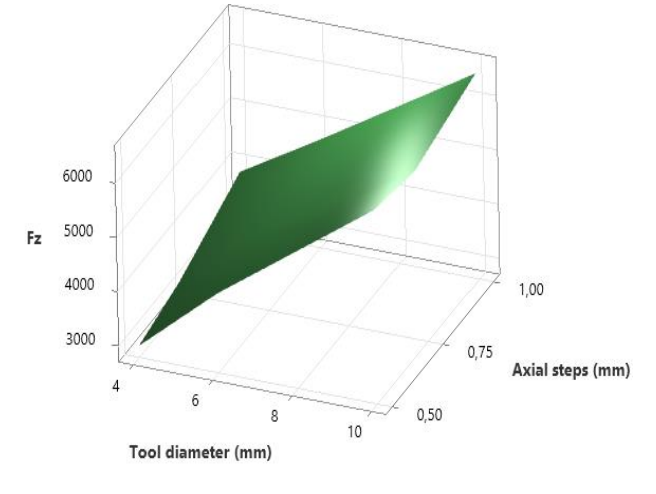
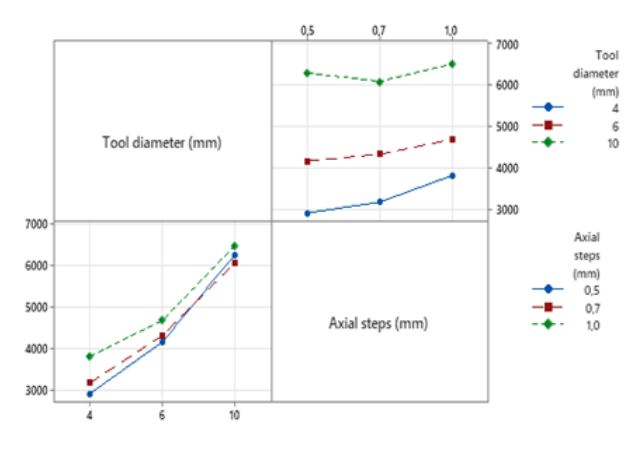
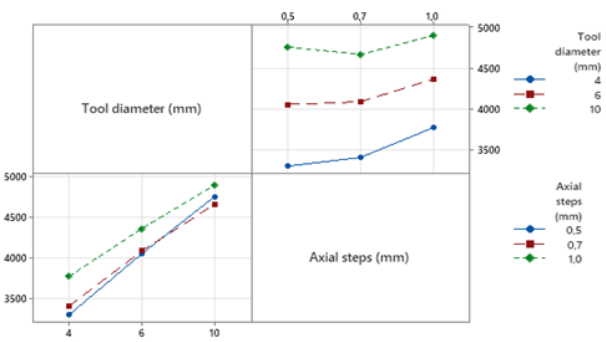


Fig. 20: Surface plot of forming force and Axial steps (mm); Tool diameter





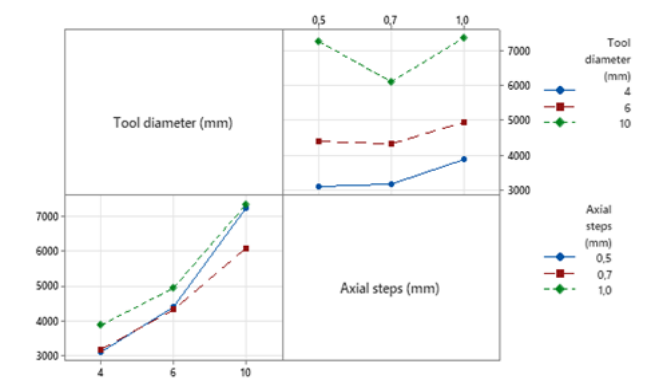


Fig. 21: Interaction effects of the input parameters on Forming force: a) Fx interaction diagram b) Fy interaction diagram c) Fz interaction diagram

It would be interesting to plot the RMS error as a function of the ratio (d/axial steps). Fig. 22 shows a trend indicating an optimum at a ratio of approximately 12. Additionally, it is noted that point 5 has the lowest error, while point 9 has the highest error. Furthermore, it could be observed that the level of RMS error remains relatively constant (around 0.15), except for point 9.

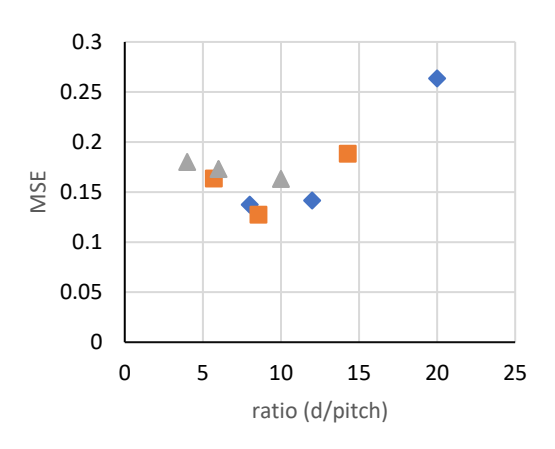


Fig. 22: Mean square error evolution

The graphs illustrated in Figs. 23, 24, and 25 show the evolution over time of the maximum forming force exerted by the tool being used. These variations are presented for different step values, namely $\Delta z=0.5$ mm, 0.7 mm, and 1 mm, along with a varying tool diameter of d=4 mm, d=6 mm, and d=10 mm, respectively. Two observations can be made from the different curves in these figures: Firstly, the axial step ΔY has no significant influence on the reaction of the forces in the deformed part. Secondly, the evolution curves of the forces appear to have similar shapes for different ΔY values and different tool diameters.

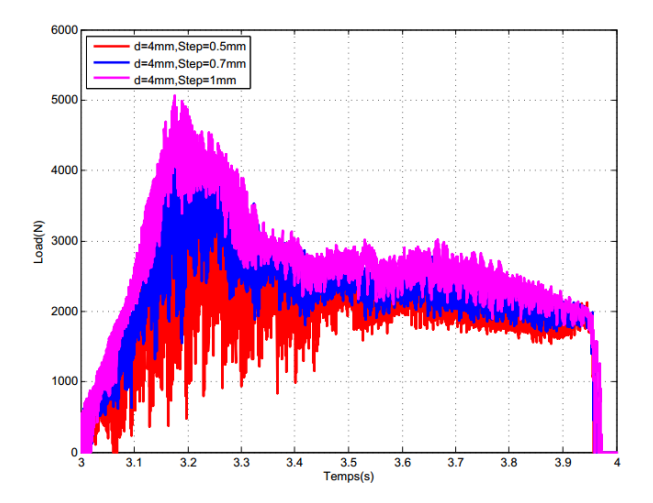


Fig. 23: Evolution of the forming force at different axial steps (0.5, 0.7, 1mm) with a tool diameter d = 4 mm

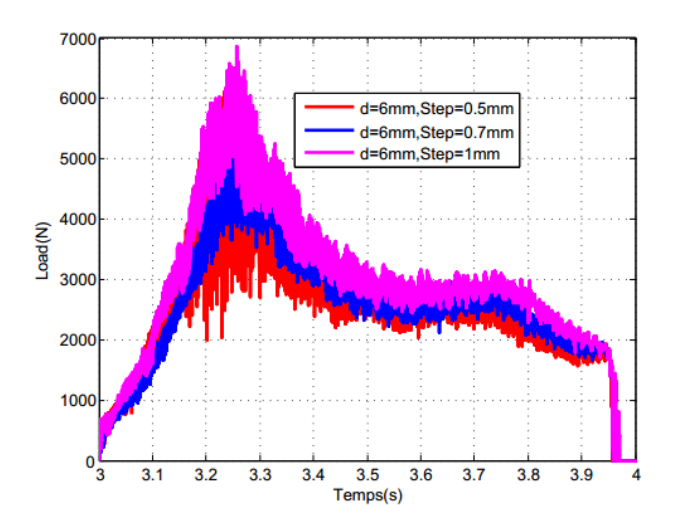


Fig. 24: Evolution of the forming force at different axial steps (0.5, 0.7, 1mm) with a tool diameter d = 6 mm

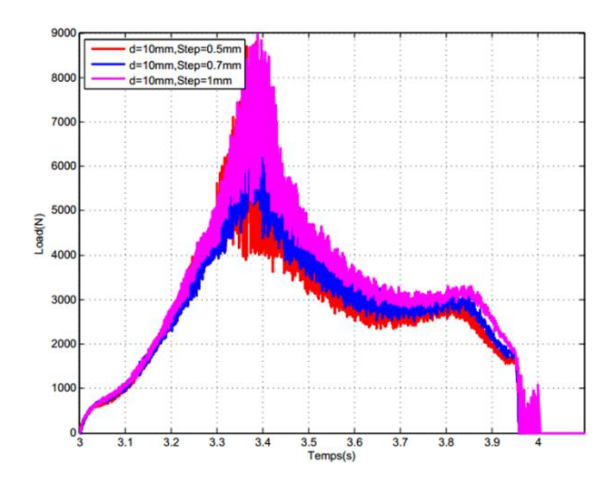


Fig. 25: Evolution of the forming force at different axial steps (0.5, 0.7, 1mm) with a tool diameter d = 10 mm

Effect of tool diameter on the distribution of forces.

The graphs in Figs. 26, 27, and 28 illustrate the evolution of the forming force applied by the tool over time for different constant vertical pitches (0.5 mm, 0.7 mm, and 1 mm) and varying tool diameters (4 mm, 6 mm, and 10 mm). We observe that reducing the diameter of the forming tool results in a decrease in the forces generated during the forming process.

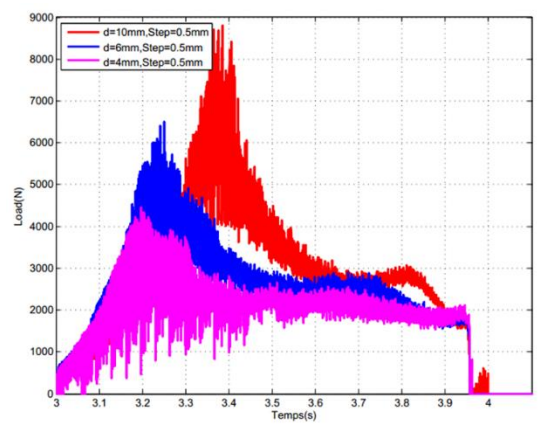


Fig. 26: Evolution of the forming force at different tool diameters d= 4, 6, 10 mm with a fixed axial steps $\Delta Z = 0.5$ mm

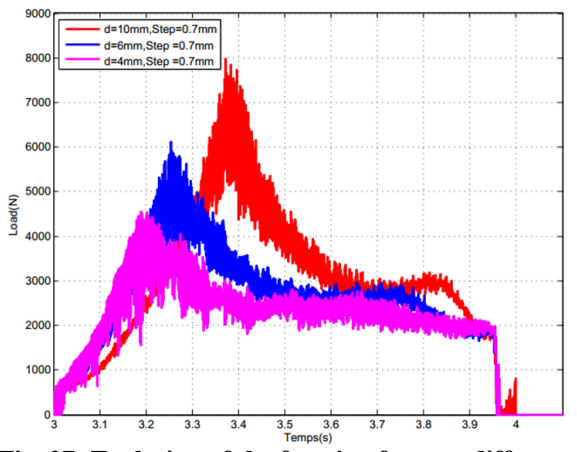


Fig. 27: Evolution of the forming force at different tool diameters d= 4, 6, 10 mm with a fixed axial steps $\Delta Z = 0.7$ mm

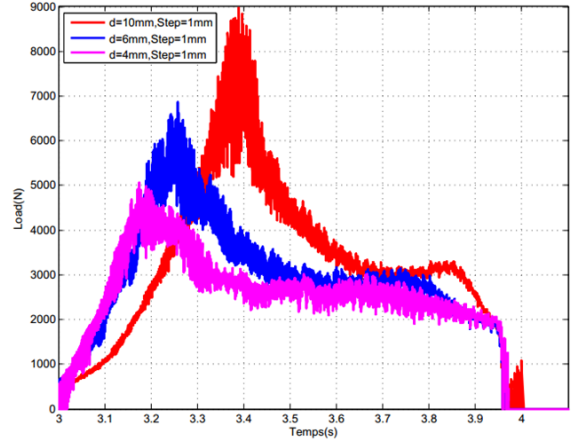


Fig. 28: Evolution of the forming force at different tool diameter d=4, 6, 10 mm with a fixed axial steps $\Delta z=1$ mm

Effect of forming angle on the distribution of forces.

Figs. 29 and 30 describe the influence of the forming rake angle, which represents an important factor in generating the force required to shape the desired form. We observe that the maximum force depends on the forming angle. Fig. 23 shows that the horizontal force exceeds the axial force in the region where the angle is significant. This result indicates that the horizontal reaction is more significant compared to the axial force. This reaction leads to elastic springback in the part geometry, which suggests that the forming angle plays a more significant role in influencing both the force exerted and the elastic springback. In conclusion, the forming angle and forming tool diameter influence the horizontal force, while the axial displacement Δz influences the axial force.

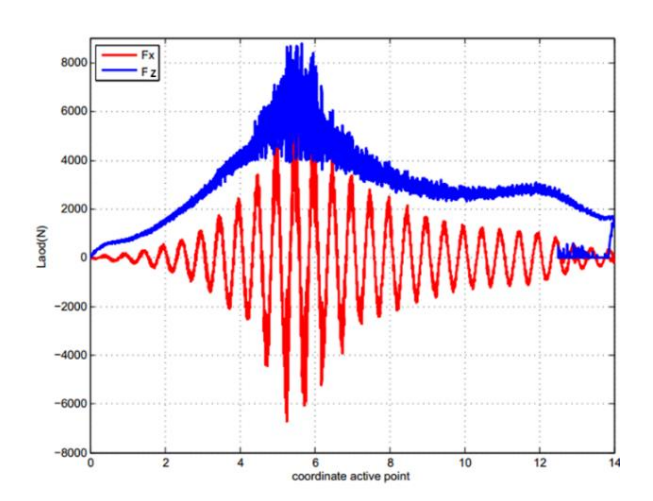


Fig. 29: Evolution of the reaction force applied to the forming tool as a function of the coordinate point

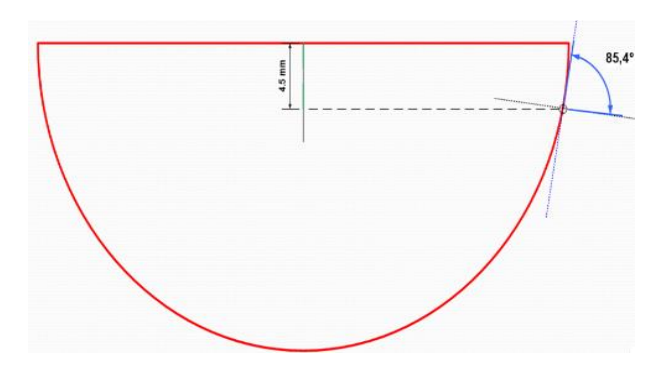


Fig. 30: Position of the maximum forming angle

5.3 Reduction in the thickness of the sheet metal

The final product geometry is crucial to the numerical simulation of the incremental forming process. Ensuring a satisfactory and reliable geometry is critical in practical applications, particularly in fields where factors such as force and pressure can contribute to part failure. It is therefore essential to study and understand the phenomenon of sheet thinning.

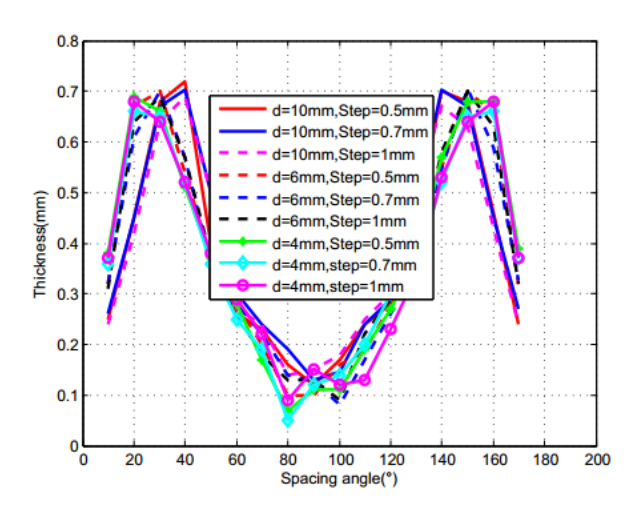


Fig. 31: Changes in sheet thickness under various conditions (d= 4, 6, 10 mm) (Δz =0.5, 0.7, 1mm)

Fig. 31 illustrates the distribution of the workpiece thickness and how it is influenced by changes in tool diameter, axial steps, and tool path. The figure illustrates the comparative evolution of sheet thickness for different tool diameters (d = 4 mm, 6 mm, and 10 mm) at various axial steps ($\Delta z = 0.5$ mm, 0.7 mm, and 1 mm). The results obtained from the three thickness distribution curves and the maximum shaping angle curve show that the minimum thickness is at the maximum angle of inclination, confirming the validity of the sine law.

5.4. Evolution of springback

In incremental forming, springback refers to the tendency of a formed part to partially return to its original shape once the forming load has been removed. When a load is applied, the material undergoes plastic deformation, which modifies its shape. However, when the load is released, the material can partially return to its original shape, thanks to its elastic properties. This elastic return can be influenced by several factors, such as the force exerted by the forming tool and the clamping force.

Effect of clamping force

The positioning of the part for forming is achieved using a die and a clamping device. The clamping device applies pressure to the edge of the part; however, when released, there is minimal relief on the edge, resulting in a very slight springback. The curve in Fig. 32 illustrates a comparison of the product geometry before and after release, as well as the desired shape.

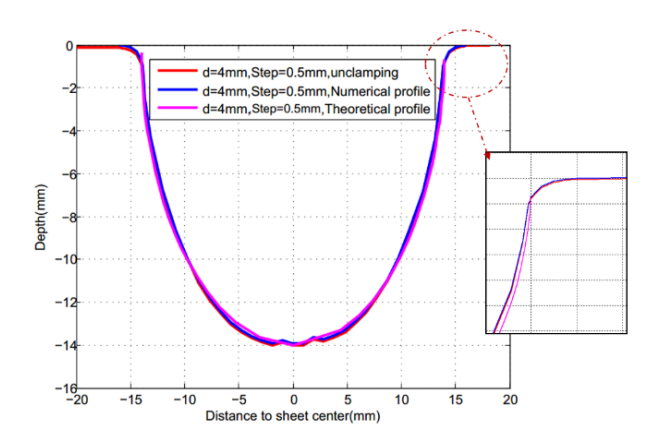


Fig. 32: Comparison of simulated profile before and after release

Springback caused by the forming tool force

Springback, caused by the force exerted by the tool in incremental forming, is the phenomenon whereby the formed part tends to partially return to its initial shape after the force has been applied by the punch. The intensity and direction of this force can significantly impact the extent of springback observed. Higher forces applied by the forming tool generally result in greater plastic deformation and, consequently, more pronounced springback. Additionally, the distribution of the tool force over the part surface can also affect the magnitude of springback. The curve in Fig. 32 illustrates springback in the zone of maximum applied stress

6. Conclusion

In this study, numerical simulations of the incremental forming process were conducted to investigate the effects of specific crucial parameters, including tool diameter, depth of cut, and tool trajectory, on force development and sheet metal thinning. The main results obtained are:

i. The geometric quality of the part is sensitive to the ratio of forming tool diameter to axial

- displacement. An optimum ratio is between 8 and 8.5, indicating that the balance between these two parameters is crucial to achieve good part geometric quality.
- ii. The force exerted during the forming process depends on several factors, including the axial steps, forming tool geometry, and the dimensions of the part being formed. The ratio between forming tool size, axial pitch, and resulting part size varies from 0.07 to 0.14. This ratio determines the amount of force required to perform the deformation. The thinning of sheet metal is influenced by the number of contact points between the part and the punch, as well as the angle of attack. An increased number of contact points and a higher angle of attack contribute to greater thinning.
- iii. A wear zone was observed at the top of the punch. Numerical simulations have shown that the hemispherical shape of the forming tool leads to thinning at the part's edge and thickening at its top. This geometric distribution reduces wear, especially when the tolerance interval's geometry is small.

In summary, numerical simulations have highlighted the importance of parameters such as the forming tool diameter ratio, axial displacement, forming tool geometry, formed part size, number of contact points, and angle of attack on part geometric quality, applied force, and sheet metal thinning. The obtained results can be used to optimize the incremental forming process and achieve higher-quality parts.

References

- P. Triclot and F. Gouin, "Mise au point-«La grosse tête»: est-ce la solution au problème de la luxation de la prothèse de hanche?," Revue de chirurgie orthopédique et traumatologique, vol. 97, no. 4, pp. S120–S127, 2011.
- H. Bergvinsson, M. Sundberg, and G. Flivik, "Polyethylene wear with ceramic and metal femoral heads at 5 years: a randomized controlled trial with radiostereometric analysis," The Journal of Arthroplasty, vol. 35, no. 12, pp. 3769–3776, 2020.
- 3. M. Ali, M. Al-Hajjar, J. Fisher, and L. M. Jennings, "Wear and deformation of metal-on-polyethylene hip bearings under edge loading conditions due to variations in component positioning," Biotribology, vol. 33, p. 100238, 2023
- 4. K. Bensaid, R. Souissi, A. Boulila, M. Ayadi, and N. Ben Fredj, "Numerical investigation of incremental forming process of AISI 304 stainless steel," Ironmaking & Steelmaking, vol. 50, no. 2, pp. 174–183, 2023.

Journal of Manufacturing Engineering, September 2025, Vol. 20, Issue. 3, pp 122-135 DOI: https://doi.org/10.37255/jme.v20i3pp122-135

- Y. Li, Z. Liu, W. Daniel, and P. Meehan, "Simulation and experimental observations of effect of different contact interfaces on the incremental sheet forming process," Materials and Manufacturing Processes, vol. 29, no. 2, pp. 121–128, 2014.
- B. Saidi, L. Giraud-Moreau, A. Cherouat, and R. Nasri, "Experimental and numerical study on optimization of the single point incremental forming of AINSI 304L stainless steel sheet," in Journal of Physics: Conference Series, IOP Publishing, 2017, p. 012039.
- T. Cao et al., "An efficient method for thickness prediction in multi-pass incremental sheet forming," The International Journal of Advanced Manufacturing Technology, vol. 77, pp. 469–483, 2015.
- 8. J. Jeswiet et al., "Asymmetric single point incremental forming of sheet metal," CIRP Annals, vol. 54, no. 2, pp. 88–114, 2005.
- 9. B. Saidi, A. Boulila, M. Ayadi, and R. Nasri, "Experimental force measurements in single point incremental sheet forming SPIF," Mechanics & Industry, vol. 16, no. 4, p. 410, 2015
- J. Duflou, Y. Tunckol, A. Szekeres, and P. Vanherck, "Experimental study on force measurements for single point incremental forming," Journal of Materials Processing Technology, vol. 189, nos. 1–3, pp. 65–72, 2007.
- C. Reddy, "Experimental and numerical studies on formability of stainless steel 304 in incremental sheet metal forming of elliptical cups," International Journal of Scientific & Engineering Research, vol. 8, no. 1, pp. 971– 976, 2017.
- 12. R. Alavala, "FEM analysis of single point incremental forming process and validation with grid-based experimental deformation analysis," International Journal of Mechanical Engineering, vol. 5, no. 5, pp. 1–6, 2016.
- R. Alavala, "Validation of single point incremental forming process for deep drawn pyramidal cups using experimental grid-based deformation," International Journal of Engineering Sciences & Research Technology.
- Y. Kim and J. Park, "Effect of process parameters on formability in incremental forming of sheet metal," Journal of Materials Processing Technology, vol. 130, pp. 42–46, 2002
- 15. J. Jeswiet and D. Young, "Forming limit diagrams for single-point incremental forming of aluminium sheet," Proceedings of the Institution of Mechanical Engineers, Part B: Journal of Engineering Manufacture, vol. 219, no. 4, pp. 359–364, 2005.
- 16. G. Ambrogio et al., "Application of incremental forming process for high customised medical product manufacturing," Journal of Materials Processing Technology, vol. 162, pp. 156–162, 2005.
- 17. S. Chezhian Babu and V. S. Senthil Kumar, "Experimental studies on incremental forming of stainless steel AISI 304

- sheets," Proceedings of the Institution of Mechanical Engineers, Part B: Journal of Engineering Manufacture, vol. 226, no. 7, pp. 1224–1229, 2012.
- G. Ambrogio, J. Duflou, L. Filice, and R. Aerens, "Some considerations on force trends in incremental forming of different materials," in AIP Conference Proceedings, American Institute of Physics, 2007, pp. 193–198.
- W. B. Abdelkader, R. Bahloul, and H. Arfa, "Numerical investigation of the influence of some parameters in SPIF process on the forming forces and thickness distributions of a bimetallic sheet CP-titanium/low-carbon steel compared to an individual layer," Procedia Manufacturing, vol. 47, pp. 1319–1327, 2020.
- 20. G. Ambrogio, L. Filice, and F. Micari, "A force measuring based strategy for failure prevention in incremental forming," Journal of Materials Processing Technology, vol. 177, nos. 1–3, pp. 413–416, 2006.
- 21. G. Hussain et al., "Tool and lubrication for negative incremental forming of a commercially pure titanium sheet," Journal of Materials Processing Technology, vol. 203, nos. 1–3, pp. 193–201, 2008.
- M.-A. Malahias et al., "Complete wear-through of a metalbacked acetabular cup in an ambulatory patient," Arthroplasty Today, vol. 5, no. 4, pp. 394–400, 2019.
- Aherwar, A. K. Singh, and A. Patnaik, "Current and future biocompatibility aspects of biomaterials for hip prosthesis," AIMS Bioengineering, vol. 3, no. 1, 2015.
- 24. M. Ham and J. Jeswiet, "Single point incremental forming and the forming criteria for AA3003," CIRP Annals, vol. 55, no. 1, pp. 241–244, 2006.
- 25. Alruhban, Contribution à l'analyse de la déformabilité de renforts tricotés, Lille 1, 2013.
- Z. Cheng et al., "Incremental sheet forming towards biomedical implants: A review," Journal of Materials Research and Technology, vol. 9, no. 4, pp. 7225–7251, 2020.
- 27. Nasulea and G. Oancea, "Incremental deformation: A literature review," in MATEC Web of Conferences, EDP Sciences, 2017, p. 03017.
- 28. T. J. Grimm and L. Mears, "Investigation of a radial toolpath in single point incremental forming," Procedia Manufacturing, vol. 48, pp. 215–222, 2020.
- 29. L. B. Said, J. Mars, M. Wali, and F. Dammak, "Effects of the tool path strategies on incremental sheet metal forming process," Mechanics & Industry, vol. 17, no. 4, p. 411, 2016.
- Kumar, V. Gulati, P. Kumar, and H. Singh, "Forming force in incremental sheet forming: a comparative analysis of the state of the art," Journal of the Brazilian Society of Mechanical Sciences and Engineering, vol. 41, pp. 1–45, 2019.

www.smenec.org 135 © SME